A Novel Neural Second-Order Sliding Mode Observer for Robust Fault Diagnosis in Robot Manipulators

Mien Van[1], Hee-Jun Kang[2,#], and Young-Soo Suh[2]

1 Graduate School of Electrical Engineering, University of Ulsan, Ulsan, South Korea, 680-749
2 School of Electrical Engineering, University of Ulsan, Ulsan, South Korea, 680-749
Corresponding Author / E-mail: hjkang@ulsan.ac.kr, TEL: +82-52-259-1635, FAX:+82-52-259-1686

This paper investigates an algorithm for fault diagnosis in robot manipulators using a novel neural second-order sliding mode observer. Differently from the conventional neural network observer and first-order sliding mode observer for the robust fault estimation schemes, the second-order sliding mode observer is first designed and compared with them. Although the second-order sliding mode observer converges faster and with less error than each of the neural network and the first-order sliding mode observer does, it requires prior knowledge of the upper bound of the fault function. Because of this disadvantage, a neural second-order sliding mode observer is designed, which combines the second-order sliding mode observer with the neural network observer. The resulting observer not only preserves the features of the second-order sliding mode observer but also can improve it by removing the need for prior knowledge of the fault function upper bound. Computer simulation results for a PUMA560 industrial robot are also shown to verify the effectiveness of the proposed strategy.

NOMENCLATURE

FD = Fault diagnosis
FDI = Fault detection and isolation
NN = Neural network
SM = Sliding mode
SOSM = Second-order sliding mode
NSOSM = Neural second-order sliding mode
EOI = Equivalent Output Injection

1. Introduction

Robotic systems are widely used in processing and manufacturing industries to improve product quality. However, some applications lead to robots being placed in hazardous and remote environments that can lead to robot failures, which can not only deteriorate product quality but also cause harm to users, and other objects in the workspace. For this reason, robot fault diagnosis is very important to the effective use of robots in manufacturing environments.

One of the advantages of robust fault diagnosis is that the systems are not only able to detect the occurrence of a fault, but also can provide information on the fault that is useful in compensating for its effects in the dynamic systems. Thus, one issue in the design of the online fault estimators is in achieving more accurate fault estimation. This expectation motivates us to develop additional approaches to fault estimation for fault diagnosis systems.

Various approaches to fault diagnosis in nonlinear systems and robot manipulators have recently been proposed. One approach using an observer based on model-based method has been explored.[1,2] Robust fault detection schemes for nonlinear systems[3-6] and robot manipulators[7-11] have also been developed using neural network (NN) learning. The basic idea of these methods is to design a robust fault diagnosis scheme using a model-based method and to then use the NN to approximate the faults in the observer design; however, the disadvantage of this method is that the fault estimation error is often quite large and the convergence time is quite slow.

It is well known that the main advantage of using sliding mode technique[12-15] is strong robustness with respect to the system uncertainties and has a fast transient response so that the observer error is smaller and the convergence time is faster. But this type of observer has two disadvantages: it provides the chattering and it requires prior

knowledge of the upper bound of the unknown input for sliding gains selection. It is a critical and possibly limiting requirement in some applications. In order to avoid chattering, many different approaches[14-26] have been proposed. They are the use of a higher order sliding mode,[19-21] the sub-optimal algorithm,[22] the super-twisting algorithm proposed for velocity observer[23,24,29] and fault diagnosis applications.[25,26] To remove the requirement that the upper bound of the unknown function be known, a neural sliding mode observer which combines NN and SM could be a good solution due to the capability of the NN to approximate the nonlinear function.

In order to solve both chattering and prior knowledge of the upper bound of the unknown function, we propose a novel neural second-order sliding mode (NSOSM) observer for robust fault diagnosis. The NSOSM observer is designed with the following principles: 1) the sliding gains are pre-selected to guarantee that there is little chattering. In this case, we can imagine that the sliding mode gains were chosen based on a "selected upper bound" of the unknown nonlinear function. 2) if the upper bound of the unknown nonlinear function is smaller than the selected upper bound value, then only the SOSM observer is activated and the system works as a conventional SOSM observer, 3) if the unknown nonlinear function surpasses the selected upper bound value, the SOSM observer is "broken, enabling activation of the NN to compensate for the SOSM estimation error.

The remainder of this paper is organized as follows: in section 2, the robot dynamics and faults are investigated and problems are described. In section 3, the fault detection scheme is designed. Three fault diagnosis schemes are described and compared in section 4, including SOSM, NN, and NSOSM observers. Computer simulation results on a PUMA560 robot are provided in section 5 to verify the effectiveness of the proposed algorithm. Section 6 outlines some conclusions.

2. Problem formulation

Consider the robot dynamics described by

$$\ddot{q} = M^{-1}(q)[\tau - V_m(q,\dot{q})\dot{q} - F(\dot{q}) - G(q) - \tau_d] + \gamma(t-T_f)\phi(q,\dot{q},\tau) \quad (1)$$

where $q \in \Re^n$ is the state vector, $\tau \in \Re^n$ is the torque produced by the actuators, $M(q) \in \Re^{n \times n}$ is the inertia matrix, $V_m(q,\dot{q}) \in \Re^n$ includes the Coriolis and centripetal forces, $F(\dot{q}) \in \Re^n$ is the friction matrix, $\tau_d = \Re^n$ is a load disturbance matrix and $G(q) \in \Re^n$ is the vector of gravity terms. The term $\phi(q,\dot{q},\tau)(\dot{q}) \in \Re^n$ is a vector representing the faults, composed of actuator faults and robot manipulator component faults, $\gamma(t-T_f) \in \Re^n$ represents the time profile of the faults, and T_f is the time of occurrence of the faults.

We let the fault time profile $\gamma(\cdot)$ be a diagonal matrix of the form

$$\gamma(t-T_f) = diag\{\gamma_1(t-T_f), \gamma_2(t-T_f), \ldots, \gamma_n(t-T_f)\} \quad (2)$$

where γ_i is a fault function that represents the fault affecting the state equation.

The faults with time profiles modeled are given by

$$\gamma_i(t-T_f) = \begin{cases} 0, & if \ t < T_f \\ 1-e^{-\varphi_i(t-T_f)} & if \ t \geq T_f \end{cases} \quad (3)$$

where $\varphi_i > 0$ represents the unknown fault evolution rate. Small φ_i values characterize slowly developing faults, also called incipient faults. For large values of φ_i, the profile of γ_i approaches a step function that models abrupt faults. When $\varphi_i \to \infty$, the γ_i becomes a step function so that incipient fault becomes an abrupt faults.

In this paper, we develop a robust fault diagnosis algorithm for robotic systems with modeling uncertainties that satisfy the following assumptions:

Assumption 1: The system states of eq. (1) for fault diagnosis (FD) and controls are bounded for all time.

Assumption 2: The modeling uncertainty is bounded by

$$\left\| M^{-1}(q)[F(\dot{q})+\tau_d] \right\| = \|\mu\| \leq \overline{\mu} \quad (4)$$

where $\overline{\mu}$ is the known constant.

The computed torque controller that is used to control the robot described by eq. (1) follows the desired trajectory. The structure of the computed torque controller is designed as

$$\tau(t) = M(q)[\ddot{q}_d + K_p(q_d-q) + K_d(\dot{q}_d-\dot{q})] + V_m(q,\dot{q})\dot{q} + G(q) \quad (5)$$

where $q_d \in \Re^n$ is the desired manipulator trajectory, K_p is the proportional gain matrix, and K_d is the derivative gain matrix.

To simplify the design, the robot dynamics can be rewritten as

$$\ddot{q} = M^{-1}(q)[\tau - V_m(q,\dot{q})\dot{q} - G(q)] \\ + M^{-1}(q)[-F(\dot{q})-\tau_d] + \gamma(t-T_f)\phi(q,\dot{q},\tau) \quad (6)$$

and if we let $x = \dot{q}^T$, the robot dynamic expressed in eq. (6) can be further simplified as

$$\dot{x} = f(q,\dot{q},\tau) + \mu(q,\dot{q},\tau) + \gamma(t-T_f)\phi(q,\dot{q},\tau) \quad (7)$$

where $f(q,\dot{q},\tau) = M^{-1}(q)[\tau - V_m(q,\dot{q})\dot{q} - G(q)]$ represents the known nominal robot dynamics. $\mu(q,\dot{q},\tau) = M^{-1}(q)[-F(\dot{q})-\tau_d]$ represents the uncertainties in the nominal model.

3. Fault detection scheme

In this section, a fault detection scheme is designed for monitoring fault occurrences. In order to detect any changes in the systems dynamics due to faults, the estimated model is compared with a nominal model. A measure of the deviation between the estimated and the nominal model give the residual.

Considering an observer of the form:

$$\dot{\hat{x}} = A(\hat{x}-x) + f(q,\dot{q},\tau) \quad (8)$$

where $\hat{x}$ is the estimation of x and A is the stable matrix that can be achieved by simply letting $A = diag(-\lambda_1, -\lambda_2, \ldots, -\lambda_n)$ with $\lambda_i > 0$.

The estimation error is obtained by substituting eq. (7) into eq. (8),

$$\dot{\tilde{x}} = A\tilde{x} + \mu(q,\dot{q},t) + \gamma(t-T_f)\phi(q,\dot{q},\tau) \quad (9)$$

where $\tilde{x} = x - \hat{x}$. Considering that when $t < T_f$, according to eq. (3)

$\gamma(t-T_f)\phi(q,\dot{q},\tau)=0$. By solving the differential equation eq. (9) with the initial condition $\tilde{x}(0)=0$, we have

$$\tilde{x}(t)=e^{At}\tilde{x}(0)+\int_0^t e^{A(t-\tau)}\mu(t)d\tau \qquad (10)$$

And with eq. (4),

$$\|\tilde{x}(t)\|\le\int_0^t e^{A(t-\tau)}\overline{\mu}(t)d\tau$$
$$=\tilde{x}_M$$

where $\tilde{x}_M$ is the chosen threshold bound. Faults are detected whenever the estimation error component $\|\tilde{x}(t)\|$ surpasses its corresponding threshold bound $\tilde{x}_M$.

4. Fault diagnosis scheme

In this section, three fault diagnosis schemes using NN, SOSM and NSOSM observers are each described. First, two fault diagnosis observer schemes based on NN and SOSM observer is described, respectively. The advantages and disadvantages of each scheme are given. Then, based on the advantages and disadvantages of each conventional scheme, a novel neural second-order sliding mode observer which combines the SOSM observer with the NN observer is designed.

4.1 Fault diagnosis observer scheme using neural network observer

For the fault system expressed in eq. (7), a NN-based fault diagnosis scheme is designed as

$$\hat{\dot{x}}=A(\hat{x}-x)+f(q,\dot{q},\tau)+\eta(t-T_f)\hat{N}(t) \qquad (11)$$

where $\hat{N}(t)$ is the online fault estimator vector. $T_k>T_f$ is the starting time that enables $\hat{N}(t)$ and operates as follows:

$$\eta(t-T_k)=\begin{cases}0, & if\ \tilde{x}<\tilde{x}_M\\1, & if\ \tilde{x}\ge\tilde{x}_M\end{cases} \qquad (12)$$

The dynamic neural network-based online estimator is chosen to be a three layer neural network. Its structure can be described by

$$\hat{N}(t)=\hat{W}\sigma(\hat{V}\bar{x}(t)) \qquad (13)$$

where $\bar{x}(t)=[q,\dot{q},\tau]^T$ is the NN input, $\hat{W},\hat{V}$ are the weight parameters, and σ is a sigmoid activation function.

The estimation error in the fault situation $(t>T_f)$ then becomes

$$\dot{\tilde{x}}=A\tilde{x}+\mu(q,\dot{q},\tau)+\phi(q,\dot{q},\tau)-\hat{W}\sigma(\hat{V}\bar{x}(t)) \qquad (14)$$

The initial weights $\hat{W},\hat{V}$ are chosen such that $\hat{W}\sigma(\hat{V}\bar{x}(t))=0$, corresponding to the fault-free case. This can be achieved simply by setting the weights of the NN output layer to zero. Starting from these initial conditions, we need to adjust the neural weights that minimize the L_2norm distance between $\phi(q,\dot{q},\tau)$ and $\hat{W}\sigma(\hat{V}\bar{x}(t))$ overall input.

In this paper, the weights tuning algorithms are taken from Refs.,[27,28] including the modified back-propagation algorithm and an e-modification term which is added to guarantee observer robustness. By choosing a cost function in the form of $J=(1/2)\tilde{x}^T\tilde{x}$, the weights tuning laws are designed as follows:

$$\hat{\dot{W}}=-\alpha_1\frac{\partial J}{\partial\hat{W}}-\rho_1\|\tilde{x}\|\hat{W} \qquad (15)$$

$$\hat{\dot{V}}=-\alpha_2\frac{\partial J}{\partial\hat{V}}-\rho_2\|\tilde{x}\|\hat{V} \qquad (16)$$

where $\alpha_1,\alpha_2>0$ are the learning rates, and $\rho_1,\rho_2>0$ are small positive numbers, the second terms on the right side of the above equations are the e-modification terms that guarantee estimation robustness in.

Based on the chain rule of derivatives, the components $(\partial J/\partial\hat{W})$ and $(\partial J/\partial\hat{V})$ can be computed by

$$\frac{\partial J}{\partial\hat{W}}=\frac{\partial J}{\partial\tilde{x}}\cdot\frac{\partial\tilde{x}}{\partial net_{\hat{W}}}\cdot\frac{\partial net_{\hat{W}}}{\partial\hat{W}}=\tilde{x}^T\cdot d_{\tilde{x}_{\hat{W}}}\cdot\frac{\partial net_{\hat{W}}}{\partial\hat{W}} \qquad (17)$$

$$\frac{\partial J}{\partial\hat{V}}=\frac{\partial J}{\partial\tilde{x}}\cdot\frac{\partial\tilde{x}}{\partial net_{\hat{V}}}\cdot\frac{\partial net_{\hat{V}}}{\partial\hat{V}}=\tilde{x}^T\cdot d_{\tilde{x}_{\hat{V}}}\cdot(\tilde{x})^T \qquad (18)$$

where $net_{\hat{W}}=\hat{W}\sigma(\hat{V}\bar{x})=\hat{N}(t)$ and $net_{\hat{V}}=\hat{V}\bar{x}$.

Based on eqs. (15) - (18), the update laws are given by

$$\hat{\dot{W}}=-\alpha_1(\tilde{x}^T d_{\tilde{x}_{\hat{W}}})^T(\sigma(\hat{V}\bar{x}))^T-\rho_1\|\tilde{x}\|\hat{W} \qquad (19)$$

$$\hat{\dot{V}}=-\alpha_2(\tilde{x}^T d_{\tilde{x}_{\hat{V}}})^T(\bar{x})^T-\rho_2\|\tilde{x}\|\hat{V} \qquad (20)$$

where

$$d_{\tilde{x}_{\hat{W}}}=\frac{\partial\tilde{x}}{\partial net_{\hat{W}}}=A^{-1},\ \frac{\partial net_{\hat{W}}}{\partial\hat{W}}=(\sigma(\hat{V}\bar{x}))^T,$$
$$d_{\tilde{x}_{\hat{V}}}=\frac{\partial\tilde{x}}{\partial net_{\hat{V}}}=A^{-1}\hat{W}(I-\Gamma(\hat{V}\bar{x}))\ and\ \Gamma(\hat{V}\bar{x})=diag\{\sigma_i^2(\hat{V}_i\bar{x})\}.$$

The stability analysis of the fault diagnosis system is given as following:

Due to the ability of NNs to approximate nonlinear functions, the unknown fault function can be described by:

$$\phi(q,\dot{q},\tau)=W\sigma(V\bar{x})+\varepsilon_1 \qquad (21)$$

where W,V are the NN's ideal weights and ε_1 is the approximation error.

We assume that the upper bounds on the optimal parameter satisfy

$$\|W\|_F\le W_M \qquad (22)$$

$$\|V\|_F\le V_M \qquad (23)$$

where $\|\cdot\|_F$ is the Frobenius norm of a matrix. Eq. (14) can be written as

$$\dot{\tilde{x}}=A\tilde{x}+\mu(q,\dot{q},\tau)+\phi(q,\dot{q},\tau)-\hat{W}\sigma(\hat{V}\bar{x})$$
$$=A\tilde{x}+\mu(q,\dot{q},\tau)+\tilde{W}\sigma(\hat{V}\bar{x})+\varepsilon_2 \qquad (24)$$

where $\tilde{W}=W-\hat{W}$ and $\varepsilon_2=W[\sigma(V\bar{x})-\sigma(\hat{V}\bar{x})]+\varepsilon_1$ because W,ε_1,σ are bounded such that $\|\varepsilon_2\|\le\overline{\varepsilon}_2$.

The stability of the fault diagnosis observer algorithm is analyzed in the following theorem:[27,28]

Theorem 1: For the robotic dynamics system expressed in eq. (7), and the proposed fault diagnosis observer scheme expressed in eq. (11), if the parameters of the NN are updated following eqs. (19) and (20), then the estimation error $\tilde{x}$ and the parameter estimation errors $\tilde{W}$ and $\tilde{V}$ are bounded.

Proof:

Let us consider a Lyapunov candidate:

$$V = \frac{1}{2}\tilde{x}^T P\tilde{x} + \frac{1}{2}tr(\tilde{W}^T\tilde{W}) \tag{25}$$

where $p = p^T$ is a positive–definite matrix which satisfies

$$A^T P + PA = -Q$$

in which Q is a positive define matrix. Based on eq. (19), we obtain

$$\dot{\tilde{W}} = \alpha_1(\tilde{x}^T d_{\tilde{x}_{\hat{W}}})^T(\sigma(\hat{V}\tilde{x}))^T + \rho_1|\tilde{x}|\hat{W} \tag{26}$$

Differentiating eq. (25), and then combining it with eqs. (24) and (26), we have

$$\dot{V} = \frac{1}{2}\dot{\tilde{x}}^T P\tilde{x} + \frac{1}{2}\tilde{x}^T P\dot{\tilde{x}} + tr(\tilde{W}^T\dot{\tilde{W}})$$
$$= -\frac{1}{2}\tilde{x}^T Q\tilde{x} + \tilde{x}^T P\mu + \tilde{x}^T P\tilde{W}\sigma(\hat{V}\tilde{x}) + \tilde{x}^T P\varepsilon_2 \tag{27}$$
$$+ tr[\tilde{W}^T\alpha_1\tilde{x}d_{\tilde{x}_{\hat{W}}}^T\sigma^T + \tilde{W}^T\rho_1|\tilde{x}|\hat{W}]$$

Based on the properties of the matrix trace and sigmoidal functions, we have

$$tr(\tilde{W}^T\alpha_1\tilde{x}d_{\tilde{x}_{\hat{W}}}^T\sigma^T) \leq |\tilde{W}|\alpha_1|\tilde{x}||d_{\tilde{x}_{\hat{W}}}|\sigma_m \tag{28}$$

$$tr(\tilde{W}^T\rho_1|\tilde{x}|\hat{W}) \leq (W_M|\tilde{W}| - |\tilde{W}|^2)\rho_1|\tilde{x}| \tag{29}$$

where σ_m is a boundary of σ: $|\sigma^T| \leq \sigma_m$.
From eqs. (27) - (29), we have

$$\dot{V} \leq -\frac{1}{2}\lambda_{\min}(Q)|\tilde{x}|^2 + |\tilde{x}||P|\bar{\mu} + |\tilde{x}||P||\tilde{W}|\sigma_m$$
$$+ |\tilde{x}||P|\bar{\varepsilon}_2 + |\tilde{W}||d_{\tilde{x}_{\hat{W}}}||\tilde{x}|\alpha_1\sigma_m$$
$$+ W_M|\tilde{W}||\tilde{x}|\rho_1 + |\tilde{W}|^2|\tilde{x}|\rho_1$$
$$= -\lambda_{hm}|\tilde{x}|^2 + \theta_2|\tilde{W}||\tilde{x}| + \theta_3|\tilde{x}| - \theta_1|\tilde{W}|^2|\tilde{x}|$$
$$\leq -\lambda_{hm}|\tilde{x}|^2 + \left(\frac{\theta_2^2}{4\theta_1} + \theta_3\right)|\tilde{x}| + \theta_1|\tilde{x}|\left(|\tilde{W}| - \frac{\theta_2}{2\theta_1}\right)^2 \tag{30}$$
$$\leq -\lambda_{hm}|\tilde{x}|^2 + \left(\frac{\theta_2^2}{4\theta_1} + \theta_3\right)|\tilde{x}|$$

where $\lambda_{\min}(Q)$ is the smallest eigenvalue of Q,

$$\lambda_{hm} = \frac{1}{2}\lambda_{\min}(Q), \theta_1 = \rho_1, \theta_2 = \sigma_m(|P| + \alpha_1|d_{\tilde{x}_{\hat{W}}}|) + W_M\rho_1$$

and $\theta_3 = \|P\|(\bar{\varepsilon}_2 + \bar{\mu})$.
Therefore, the condition to guarantee a negative $\dot{V}$ is as follows:

$$|\tilde{x}| > \frac{\theta_2^2 + 4\theta_1\theta_3}{4\theta_1\lambda_{hm}} = r \tag{31}$$

This means that $\dot{V}$ is negative definite outside the ball with radius r described as $B = \{\tilde{x}||\tilde{x}| \leq r\}$, which shows the boundary of $\tilde{x}$. From eq. (19), we show the boundary of $\tilde{W}$ with

$$\dot{\tilde{W}} = -\rho_1|\tilde{x}|\tilde{W} + \rho_1|\tilde{x}|W + \alpha_1\tilde{x}d_{\tilde{x}_{\hat{V}}}^T\sigma^T \tag{32}$$

Both the second and third terms on the right side of the linear system in eq. (32) are bounded because $\tilde{x}$, W, σ and $d_{\tilde{x}_{\hat{W}}}$ are bounded and matrix A is stable. Because ρ_1 is positive, the dynamic of eq. (32) is also stable. Consequently, $\tilde{W}$ is bounded, so $\hat{W}$ is also bounded.

Then, the bounded property of $\hat{V}$ is considered. From eq. (20), we have

$$\dot{\tilde{V}} = -\rho_2|\tilde{x}|\tilde{V} + \rho_2|\tilde{x}|V + \alpha_2\tilde{x}d_{\tilde{x}_{\hat{V}}}^T\tilde{x}^T \tag{33}$$

Because $\tilde{x}, V, d_{\tilde{x}_{\hat{V}}}$ are all bounded, the second and third terms of eq. (33) are also bounded. Additionally, α_2 and ρ_2 are positive numbers. The right side of the linear system in eq. (33) contains bounded inputs, so is therefore also bounded. (Q.E.D)

The above stability analysis demonstrates that the estimation error ($\tilde{x}$) and the resulting parameter estimation errors ($\tilde{W}$ and $\tilde{V}$) are bounded under the observer scheme expressed in eq. (11).

4.2 Fault diagnosis observer scheme using second-order sliding mode observer

In this section, a robust fault diagnosis based on the SOSM observer is designed. The observer scheme consists of a supper-twisting SOSM that is incorporated into a nonlinear observer to create a robust nonlinear observer and faults are reconstructed from the equivalent output injection (EOI) of the SM.

To design for robust fault diagnosis based on the SOSM observer, we require the following additional assumption:

Assumption 3: the unknown fault function is bounded

$$\phi(q, \dot{q}, \tau) \leq \bar{\phi} \tag{34}$$

where $\bar{\phi}$ is the known constant.

For the system expressed in eq. (7) that satisfies assumptions 1-3 and is based on Ref.,[20] the SOSM-based fault diagnosis observer is designed according to

$$\dot{\hat{x}} = A(\hat{x} - x) + f(q, \dot{q}, \tau) + \eta(t - T_k)\hat{S}(t) \tag{35}$$

where $\hat{S}(t)$ is the robust term based on the SOSM observer, and is in turn designed as

$$\hat{S}(t) = k_1|\tilde{x}|^{1/2}sign(\tilde{x}) - z$$
$$\dot{z} = -k_2 sign(\tilde{x}) \tag{36}$$

The estimation error can be obtained from eqs. (7) and (35) in the presence of the fault such that

$$\dot{\tilde{x}} = A\tilde{x} + \mu(q, \dot{q}, \tau) + \phi(q, \dot{q}, \tau) - \hat{S}(t) \tag{37}$$

Let $\psi(q,\dot{q},\tau) = A\tilde{x} + \mu(q,\dot{q},\tau) + \phi(q,\dot{q},\tau)$, such that based on assumptions 1 - 3, we have

$$\psi(q,\dot{q},\tau) \le \overline{\psi} \tag{38}$$

where $\overline{\psi}$ is a known constant.

The stability analysis below is given to demonstrate that the estimation error converges in finite time, by following:[29]

Theorem 2 For the robotic dynamics system expressed in eq. (7) and the proposed fault diagnosis observer expressed in eq. (35), if the sliding mode gains of the SOSM as expressed in eq. (36) are selected as

$$k_1 > 2\overline{\psi} \text{ and } k_2 > k_1 \frac{5k_1 + 4\overline{\psi}}{(2k_1 - 4\overline{\psi})} \overline{\psi} \tag{39}$$

then the fault estimation error $\tilde{x}$ is stable and converges to zero in finite time.

Proof

From eq. (37), the fault estimation error is expressed as

$$\dot{\tilde{x}} = \psi(q,\dot{q},\tau) - k_1 |\tilde{x}|^{1/2} sign(\tilde{x}) + z$$
$$\dot{z} = -k_2 sign(\tilde{x}) \tag{40}$$

Let us consider a Lyapunov candidate

$$L = 2k_2|\tilde{x}| + \frac{1}{2}(k_1|\tilde{x}|^{1/2}sign(\tilde{x}) - z)^2 + \frac{z^2}{2} \tag{41}$$

Eq. (41) can be written as a quadratic form:

$$L = \zeta^T P \zeta \tag{42}$$

where $\zeta = [|\tilde{x}|^{1/2}sign(\tilde{x}), z]^T$ and $P = \frac{1}{2}\begin{bmatrix} k_1^2 + 4k_2 & -k_1 \\ -k_1 & 2 \end{bmatrix}$.

Combining eqs. (40) and (42), the time derivative of L becomes

$$\dot{L} = -\frac{1}{|\tilde{x}|^{1/2}}(\zeta^T T_1 \zeta - \psi T_2 \zeta) \tag{43}$$

where $T_1 = \frac{k_1}{2}\begin{bmatrix} 2k_2 + k_1^2 & -k_1 \\ -k_1 & 1 \end{bmatrix}$ and $T_2 = \left[2k_2 + \frac{k_1^2}{2}, -\frac{k_1}{2}\right]^T$.

Recalling that $|\psi| < \overline{\psi}$, eq. (43) can be after manipulated algebraically to

$$\dot{L} \le -\frac{1}{|\tilde{x}|^{1/2}}\zeta^T T_3 \zeta \tag{44}$$

where $T_3 = \frac{k_1}{2}\begin{bmatrix} 2k_2 + k_1^2 - \left(\frac{4k_2}{k_1} + k_1\right)\overline{\psi} & -(k_1 + 2\overline{\psi}) \\ -(k_1 + 2\overline{\psi}) & 1 \end{bmatrix}$.

Under the conditions of eq. (39), T_3 becomes larger than zero ($T_3 > 0$) and then, from eq. (44), $\dot{L}$ is a negative-definite matrix, proving its stability.

In order to prove the convergence of the SOSM observer, we start with the Lyapunov function of eq. (41). Because k_1 and k_2 are positives, L is also always positive and satisfies the following condition:

$$\lambda_{min}(p)|\zeta|^2 \le L \le \lambda_{max}(p)|\zeta|^2 \tag{45}$$

where $|\zeta|^2 = |\tilde{x}| + |z|^2$ is the Euclidean norm of ζ.

Using eqs. (44) and (45) and the fact that

$$|\tilde{x}|^{1/2} \le |\zeta| \le \frac{L^{1/2}}{\lambda_{min}^{1/2}(P)} \tag{46}$$

it follows that

$$\dot{L} \le -\frac{1}{|\tilde{x}|^{1/2}}\zeta^T T_3 \zeta \le -\beta L^{1/2} \tag{47}$$

and hence,

$$\dot{L} \le -\beta L^{1/2} \tag{48}$$

where

$$\beta = \frac{\lambda_{min}^{1/2}(P)\lambda_{min}(T_3)}{\lambda_{max}(P)} > 0$$

Since the solution of the differential equations

$$\dot{y} = -\beta y^{1/2}, \; y(0) = y_0 \ge 0$$

is

$$y(t) = \left(y_0^{1/2} - \frac{\beta}{2}t\right)^2$$

Here $y(t)$ converges to zero in finite time and reaches zero after $t = \frac{2}{\beta}y_0^{1/2}$. Combining this result with the comparison principle from Ref.[30] leads to the relation $L(t) \le y(t)$ when $L(\zeta_0) \le y_0$. Therefore, $\tilde{x}(t)$ converges to zero as $L(\tilde{x}(t))$ converges to zero after $T = \frac{2}{\beta}L^{1/2}(\zeta_0)$ units of time. (Q.E.D)

4.3 Fault diagnosis scheme using a neural second-order sliding mode (NSOSM) observer

In sections 4.1 and 4.2, we designed fault diagnosis schemes using separate NN and SOSM observers. However, when using SOSM observer, prior knowledge of the unknown fault function upper bound is required (Assumption 3 in section 4.2). This is usually not a valid assumption in real-life applications. Moreover, if the upper bound of the fault function is known but large, then the selected sliding gain is too large to guarantee finite time convergence, causing undesired chattering. A neural network is a smooth function and does not require the bounds of the fault function as inputs, but the approximation error is bigger than for an SOSM observer. To overcome these drawbacks, in this section we design a fault diagnosis scheme that uses an NSOSM observer that combines the SOSM and NN observers. It is designed as follows:

$$\dot{\hat{x}} = A(\hat{x} - x) + f(q,\dot{q},\tau) + \eta(t - T_k)\hat{M}(t) \tag{49}$$

where $\hat{M}(t)$ is the online estimator vector, which is broken down to

$$\hat{M}(t) = \hat{S}(t) + s_t \hat{N}(t) \tag{50}$$

where $\hat{S}(t)$ and $\hat{N}(t)$ correspond to the SOSM and NN observers defined in the previous sections. However, the sliding gains of the SOSM observer are not chosen based on the fault function upper bound (this fault function bound is unknown). In this case, the sliding gains are selected to guarantee that the chattering is small. s_t is the switching term that allows the NN to work under the following switching condition:

$$s_t = \begin{cases} 1, & if \ |\tilde{x}| \ge \omega \\ 0, & if \ |\tilde{x}| < \omega \end{cases} \qquad (51)$$

where ω is a constant that will be defined later and allows the NN to work when the sliding motion is "broken". $\tilde{x} = x - \hat{x}$ is the estimation error and is defined when the fault occurred as following:

$$\dot{\tilde{x}} = A\tilde{x} + \mu(q, \dot{q}, \tau) + \phi(q, \dot{q}, \tau) - \hat{M}(t) \qquad (52)$$

The principle operation of NSOSM based fault diagnosis observer is illustrated in Fig. 1. In this case, the sliding mode gains were pre-selected based on the selected upper bound S in Fig. 1, to guarantee less chattering. The constant ω is designed such that when the upper bound of the occurred fault is smaller than the selected bound S (Fault 1, 2 in Fig. 1), only the SOSM observer is activated to estimate the fault function ($s_t = 0$). If the upper bound of the fault function overshoots the selected bound S (Fault 3 in the time between t_1 and t_2 in Fig. 1), then the term $s_t = 1$ is switched to enable the NN to compensate for the SOSM estimation error.

To simplify the analysis, we can divide the unknown fault function ϕ into two parts:

$$\phi(q, \dot{q}, \tau) = \phi_1(q, \dot{q}, \tau) + \phi_2(q, \dot{q}, \tau) \qquad (53)$$

where $\phi_1(q, \dot{q}, \tau)$ satisfies $\mu(q, \dot{q}, \tau) + \phi_1(q, \dot{q}, \tau) < S$ which represents the part approximated by the SOSM observer and $\phi_2(q, \dot{q}, \tau)$ represents the part approximated by the NN observer. If the upper bound of the fault ϕ is smaller than the selected bound S, then $\phi_2 = 0$, the NSOSM observer operating same as SOSM observer does. Else, the component $\phi_2 \ne 0$, based on the universal approximation ability of the NN observer, optimal parameter weights W, V exist such that

$$|\phi_2(q, \dot{q}, \tau) - W\sigma(V\bar{x}(t))| = \delta(t) < \bar{\delta} \qquad (54)$$

where $\bar{\delta}$ represents the upper bound of the neural network approximation error. The unknown input estimated by the SOSM is now $\phi_1(q, \dot{q}, \tau) = \phi_1(q, \dot{q}, \tau) + \bar{\delta} < S$, smaller than the selected bound S, making the stability and convergence analysis of this situation similar to that in section 4.2.

5. Simulation results

In order to verify the effectiveness of the proposed algorithm, its overall procedure is simulated for a PUMA560 robot, in which the first three joints are used. The PUMA robot is a well-known industrial robot that has been widely used in industrial applications and robotic
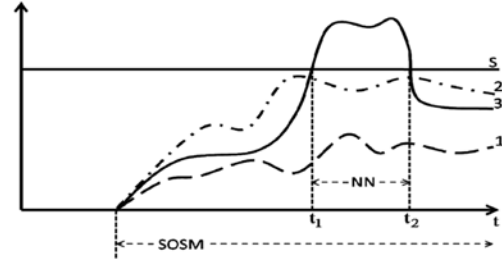

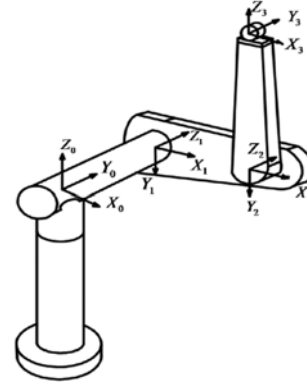Fig. 1 Faults magnitude and selected sliding mode gains

Fig. 2 D-H Coordinate frames of the 3-DOF PUMA560 robot

research. Its explicit dynamic model and the parameter values necessary to control it are given in Ref.[31]

The three degree of freedom (3-DOF) PUMA560 robot is considered with the last three joints locked. Its kinematic description is shown in Fig. 2. The uncertainties used in this simulation are given as follows:

$$F(\dot{q}) = \begin{bmatrix} 1.1\dot{q}_1 + 0.3\sin(3q_1) \\ 1.2\dot{q}_2 + 0.4\sin(2q_2) \\ 1.4\dot{q}_3 + 0.3\sin(q_3) \end{bmatrix} \qquad (55)$$

and

$$\tau_d = \begin{bmatrix} 0.2\sin(\dot{q}_1) \\ 0.1\sin(\dot{q}_2) \\ 0.15\sin(\dot{q}_3) \end{bmatrix} \qquad (56)$$

In this paper, the computed torque controller is used to control the robot following a desired trajectory. The structure of the computed torque controller has been given in eq. (5) with $K_P = 15I_{3\times3}$ and $K_d = 10I_{3\times3}$, where $I_{n\times n}$ represents an identity matrix of $n \times n$ dimensions.

In this simulation we compare the three designed observer schemes including the NN, SOSM and NSOSM observers, to verify the effectiveness of the proposed strategy. Matlab/Simulink is used to perform all the simulations. The sampling time of the simulation is set to 10^{-4}. The stable matrix $A = diag(-10, -10, -10)$. The neural network is a three-layer neural network has 30 neurons, and its tuning laws are given in eqs. (19) and (20) with $\alpha_1 = \alpha_2 = 5$, $\rho_1 = \rho_2 = 0.02$. The sliding mode gains are selected to be $k_1 = k_2 = 4$ corresponding to the pre-selected bound value S_s. The switching error is selected to be $\omega = 0.1$. In normal operation, the robot tracks to the desired trajectory. The performance is shown in Fig. 3.
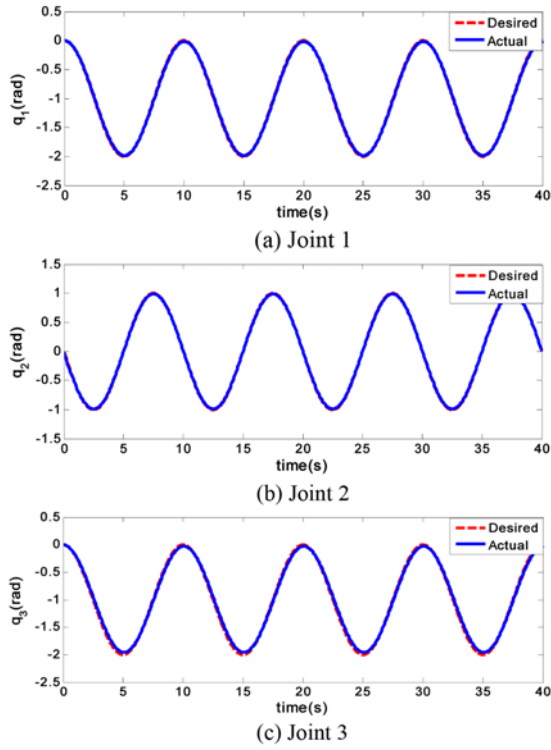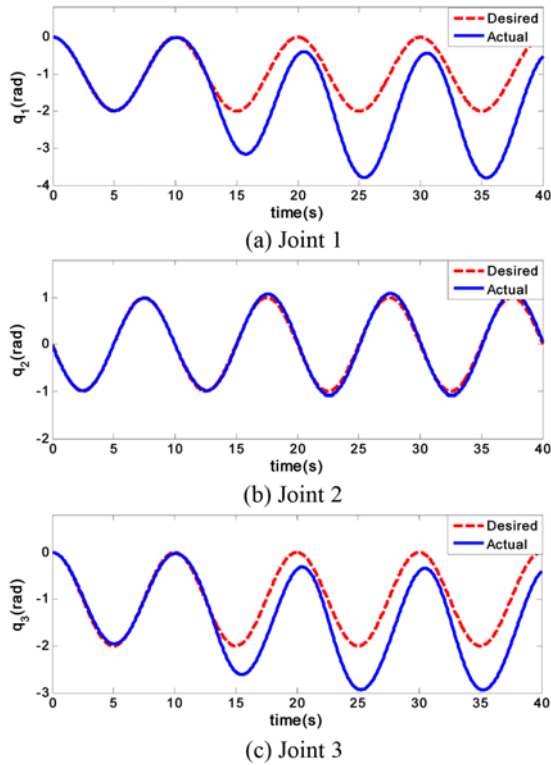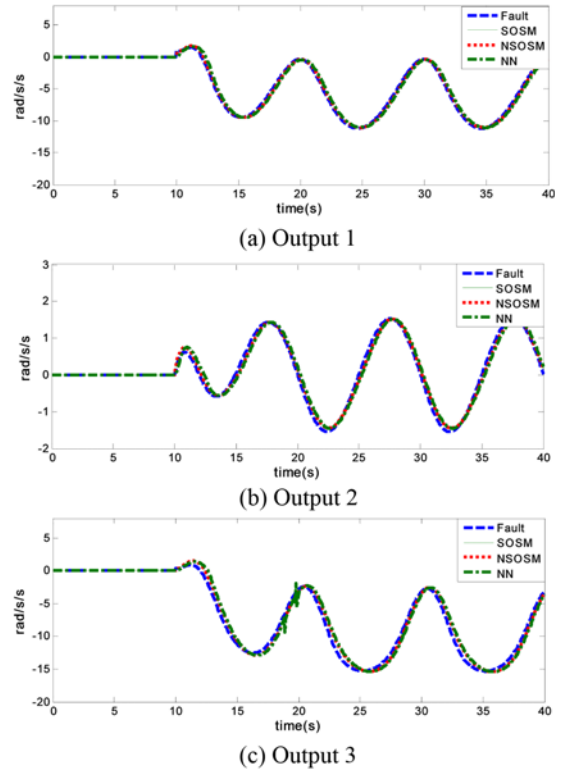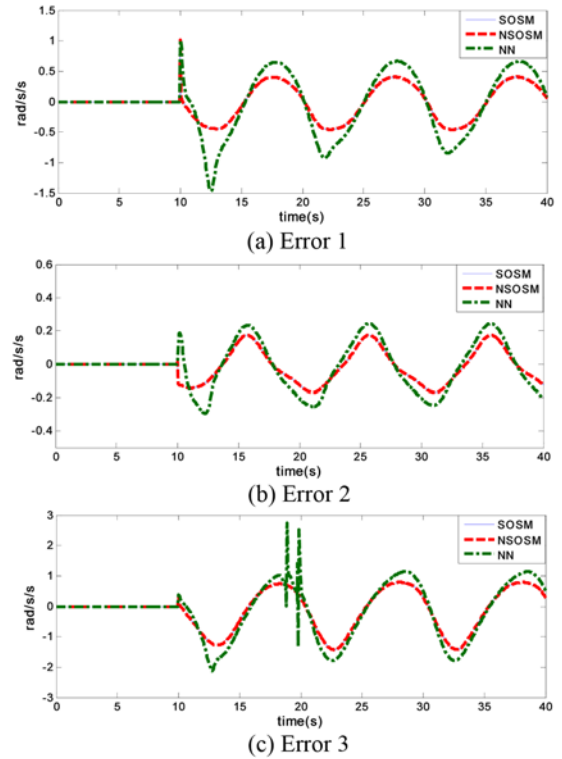
Fig. 3 Joint angle trajectories when no fault occurs

Fig. 4 Joint angle trajectories when fault ϕ_1 occurs

Fig. 5 Time histories of the fault function ϕ_1 and the SOSM, NSOSM and NN outputs when fault ϕ_1 occurs.

Fig. 6 The estimation error between the fault ϕ_1 and the outputs of the SOSM, NSOSM and NN observers

Now, let us turn to the fault estimation of the proposed algorithm. The main purpose of this simulation is to show the performance of the NSOSM observer for two types of faults: faults with an upper bound below the bound value S_s and the faults with the upper bound bigger than the bound S_s. First, we consider a fault ϕ_1 with the upper bound below the bound S_s:

$$\phi_1 = \begin{bmatrix} 10q_1^3 + 0.5\dot{q}_2 + 10q_3 \\ 1.24q_2 + 0.04\dot{q}_2 + 0.6\sin(\dot{q}_3) \\ 0.6\sin(q_1) + 5q_3 + 3\sin(q_3) \end{bmatrix} \qquad (57)$$
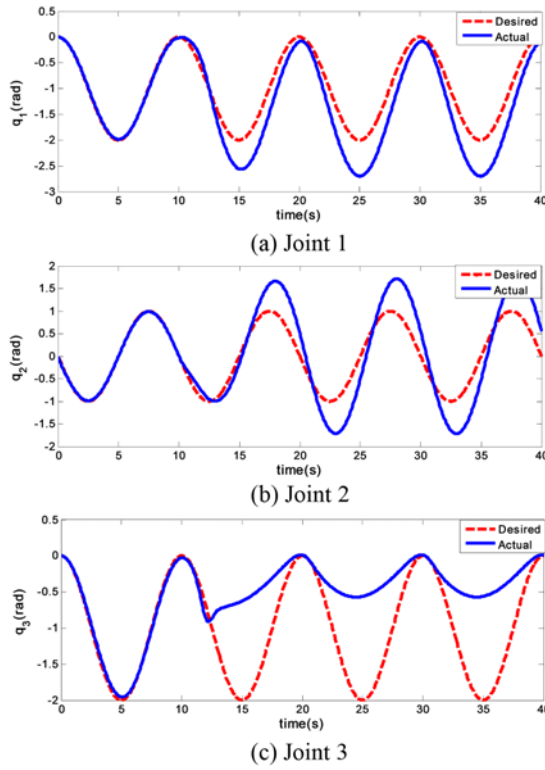
Fig. 7 Joint angle trajectories when fault ϕ_2 occurs
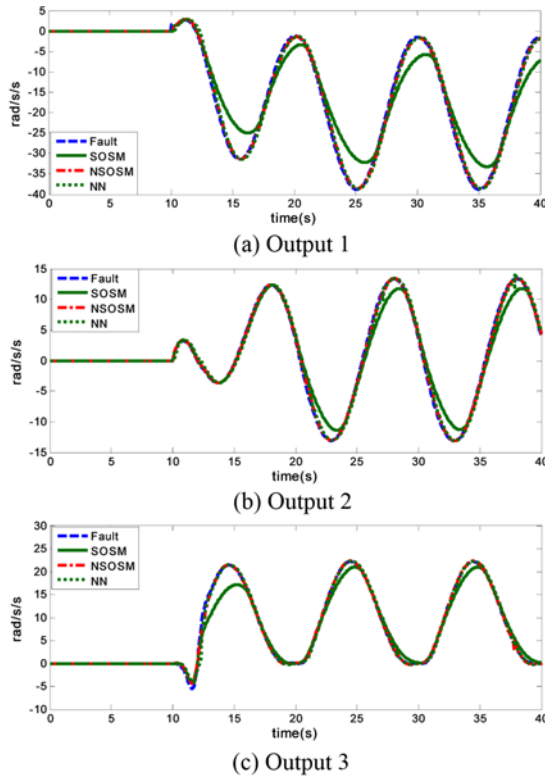
Fig. 8 Time histories of the fault function ϕ_2 and the SOSM, NSOSM and NN outputs when fault ϕ_2 occurs

The time histories of the join angles in the presence of a fault ϕ_1 at $t = 10s$ are shown in Fig. 4. It can be seen that the tracking error become larger when $t > 10s$ due to the effect of the fault ϕ_1. The fault estimation capability of each observer scheme (NN, SOSM, NSOSM)
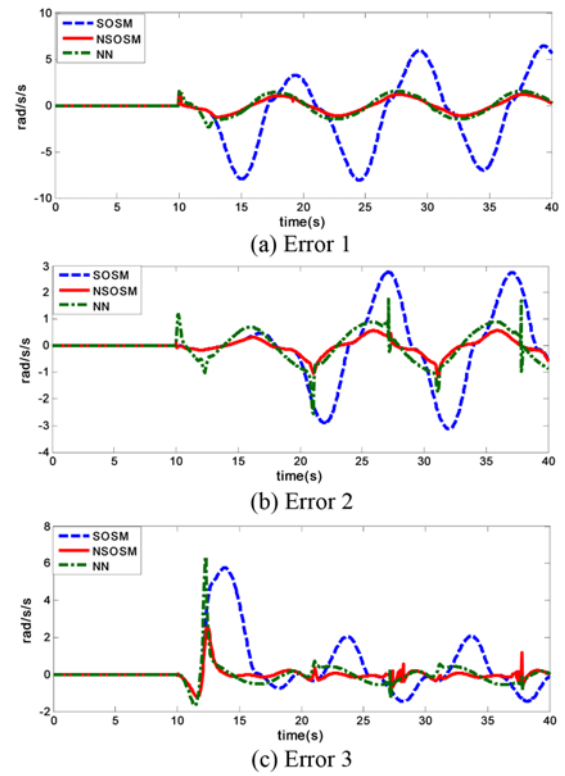
Fig. 9 The estimation error between the fault ϕ_2 and the outputs of the SOSM, NSOSM and NN observers

is shown in Fig. 5 and the corresponding detailed estimated error graph between faults and estimated faults are illustrated in Fig. 6. From these figures, we see that the NSOSM observer performs exactly same as the SOSM observer does. It means that the fault ϕ_1 effect does not exceed the selected value ω so that only the SOSM observer is able to approximate the fault function. Moreover, it also shown the convergence time of NSOSM is faster and has less error than the NN observer. The observer mismatch between the fault function and its estimated output inevitably comes from modeling uncertainties and error fault approximations of each observer.

Now, we consider a fault with the upper bound above the selected bound S_s. Let us consider a fault ϕ_2 as given below

$$\phi_2 = \begin{bmatrix} 50q_1^3 + 0.5\dot{q}_2 + 20q_3 \\ 7.44q_2 + 0.24\dot{q}_2 + 3.6\sin(\dot{q}_3) \\ 56\sin(q_1) + 70q_3^2 + 1.05\sin(q_3) \end{bmatrix} \tag{58}$$

This fault is assumed to occur at $t = 10s$. The time histories of the joint angles are shown in Fig. 7. From Figs. 8 and 9, which show the fault estimates and the detailed estimated error in the presence of fault ϕ_2, we see that the SOSM was broken, indicating that the estimation error was too large. This problem was compensated by the NN in the NSOSM observer, the estimation error is much smaller. In addition, Figs. 8 and 9 also show that the NSOSM observer keeping the transient response features of the SOSM observer so that its transient response is extremely small compare with NN response. Otherwise, the NSOSM observer has less error than the NN observer does.

These figures show two working modes of the proposed NSOSM observer corresponds to the effect of two types of faults ϕ_1 and ϕ_2 in

terms of fault approximation. In both cases, the NSOSM observer has less transient response and error than the NN observer does. Moreover, the NSOSM observer keeping the properties of the SOSM observer in the type of fault ϕ_1, and it is much better than the SOSM observer in the type of fault ϕ_2.

6. Conclusions

A robust fault diagnosis algorithm for robotic systems is proposed that models uncertainties with a neural second-order sliding mode (NSOSM) observer. The NSOSM observer could allow us to remove the requirement that the upper bound of the unknown fault function be known. This observer scheme can also reduce the chattering of the SOSM observer and lead to less estimation errors than the conventional NN observer. The convergence of the proposed neural second-order sliding mode observer was proved theoretically. The results of computer simulations for a 3-DOF PUMA560 robot, comparing the SOSM, NSOSM, and NN observers, verify the effectiveness of the proposed strategy.

REFERENCES

1. Gertler, J. J., "Survey of model-based failure detection and isolation in complex plants," Control Systems Magazine, Vol. 8, No. 6, pp. 3-11, 1988.

2. Frank, P. M. and Ding, X., "Survey of robust residual generation and evaluation methods in observer-based fault detection systems," Journal of Process Control, Vol. 7, No. 6, pp. 403-424, 1997.

3. Polycarpou, M. M. and Helmicki, A. J., "Automated fault detection and accommodation: a learning systems approach," IEEE Transactions on Systems, Man and Cybernetics, Vol. 25, No. 11, pp. 1447-1458, 1995.

4. Polycarpou, M. M. and Trunov, A. B., "Learning approach to nonlinear fault diagnosis: detectability analysis," IEEE Transactions on Automatic Control, Vol. 45, No. 4, pp. 806-812, 2000.

5. Trunov, A. B. and Polycarpou, M. M., "Automated fault diagnosis in nonlinear multivariable systems using a learning methodology," IEEE Transaction on Neural Networks, Vol. 11, No. 1, pp. 91-101, 2000.

6. Zhang, X., Parisini, T., and Polycarpou, M. M., "Sensor bias fault isolation in a class of nonlinear systems," IEEE Transactions on Automatic Control, Vol. 50, No. 3, pp. 370-376, 2005.

7. Vemuri, A. T. and Polycarpou, M. M., "Neural-network-based robust fault diagnosis in robotic systems," IEEE Transaction on Neural Networks, Vol. 8, No. 6, pp. 1410-1420, 1997.

8. Huang, S. N., Tan, K. K., and Lee, T. H., "Automated fault detection and diagnosis in mechanical systems," IEEE Transactions on Systems, Man, and Cybernetics, Part C: Applications and Reviews, Vol. 37, No. 6, pp. 1094-6977, 2007.

9. Huang, S. N. and Kok, K. T., "Fault detection, isolation, and accommodation control in robotic systems," IEEE Transaction on Automation Science and Engineering, Vol. 5, No. 3, pp. 480-489, 2008.

10. Eski, I., Erkaya, S., Savas, S., and Yildirim, S., "Fault detection on robot manipulators using artificial neural networks," Robotics and Computer-Integrated Manufacturing, Vol. 27, No. 1, pp. 115-123, 2011.

11. Van, M., Kang, H.-J., and Ro, Y.-S., "A robust fault detection and isolation scheme for robot manipulators based on neural networks," ICIC2011, LNCS 6838, pp. 25-32, Springer-Verlag, 2011.

12. Utkin, V., "Variable structure systems with sliding modes," IEEE Transactions on Automatic Control, Vol. 22, No. 2, pp. 212-222, 1977.

13. Utkin, V., "Sliding modes in control and optimizations," Springer-Verlag, Berlin, Germany, 1992.

14. Yun, D., Kim, H., and Boo, K., "Brake performance evaluation of ABS with sliding mode controller on a split road with driver model," Int. J. Precis. Eng. Manuf., Vol. 12, No. 1, pp. 31-38, 2011.

15. Dinh, V.-T., Nguyen, H., Shin, S.-M., Kim, H.-K., Kim, S.-B., and Byun, G.-S., "Tracking control of omnidirectional mobile platform with disturbance using differential sliding mode controller," Int. J. Precis. Eng. Manuf., Vol. 13, No. 1, pp. 39-48, 2012.

16. Yi, X. and Saif, M., "Sliding mode observer for nonlinear uncertain systems," IEEE Transactions on Automatic Control, Vol. 46, No. 12, pp. 2012-2017, 2001.

17. Veluvolu, K. C., Soh, Y. C., and Cao, W., "Robust observer with sliding mode estimation for nonlinear uncertain systems," IET Control Theory & Applications, Vol. 1, No. 5, pp. 1533-1540, 2007.

18. Edwards, C., Spurgeon, S. K., and Patton, R. J., "Sliding mode observers for fault detection and isolation," Automatica, Vol. 36, No. 4, pp. 541-553, 2000.

19. Levant., A., "Sliding order and sliding accuracy in sliding mode control," International Journal of Control, Vol. 58, No. 6, pp. 1247-1263, 1993.

20. Levant, A., "Robust exact differentiation via sliding mode technique," Automatica, Vol. 34, No. 3, pp. 379-384, 1998.

21. Bartolini, G., Ferrara, A., and Usai, E., "Chattering avoidance by second order sliding mode control," IEEE Transactions on

Automatic Control, Vol. 43, No. 2, pp. 241-246, 1998.

22. Brambilla, D., Capisani, L. M., Ferrara, A., and Pisu, P., "Fault Detection for Robot Manipulators via Second-Order Sliding Modes," IEEE Transactions on Industrial Electronics, Vol. 55, No. 11, pp. 3954-3963, 2008.

23. Davila, J., Fridman, L., and Levant, A., "Second-order sliding-mode observer for mechanical systems," IEEE Transactions on Automatic Control, Vol. 50, No. 11, pp. 1785-1789, 2005.

24. Davila, J., Fridman, L., and Poznyak, A., "Observation and Identification of Mechanical Systems via Second Order Sliding Modes," International Workshop on Variable Structure Systems, pp. 232-237, 2006.

25. Edwards, C., Fridman, L., and Thein, M.-W. L., "Fault Reconstruction in a Leader/Follower Spacecraft System Using Higher Order Sliding Mode Observers," Proceeding of American Control Conference, pp. 408-413, 2007.

26. Capisani, L. M., Ferrara, A., and Fridman, L., "Higher Order Sliding Mode observers for actuator faults Diagnosis in robot manipulators," IEEE International Symposium on Industrial Electronics (ISIE), pp. 2103-2108, 2010.

27. Abdollahi, F., Talebi, H. A., and Patel, R. V., "A stable neural network-based observer with application to flexible-joint manipulators," IEEE Transactions on Neural Networks, Vol. 17, No. 1, pp. 118-129, 2006.

28. Qing, W. and Saif, M., "A neural-fuzzy sliding mode observer for robust fault diagnosis," Proceeding of American Control Conference, pp. 4982-4987, 2009.

29. Moreno, J. A. and Osorio, M., "A Lyapunov approach to second-order sliding mode controllers and observers," Proceeding of 47th IEEE Conference on Decision and Control, pp. 2856-2861, 2008.

30. Khalil, H., "Nonlinear systems," Prentice Hall, New Jersey, USA, 2002.

31. Armstrong, B., Oussama, K., and Burdick, J., "The Explicit Dynamic Model and Inertial Parameters of the PUMA 560 Arm," Proceeding of 1986 IEEE International Conference on Robotics and Automation, Vol. 3, pp. 510-518, 1986.